ISSN 0038-0946, Solar System Research, 2013, Vol. 47, No. 6, pp. 454–462. © Pleiades Publishing, Inc., 2013.
Original Russian Text © Zh.M. Dlugach, M.I. Mishchenko, 2013, published in Astronomicheskii Vestnik, 2013, Vol. 47, No. 6, pp. 494–503.

Coherent Backscattering and Opposition Effects Observed in Some Atmosphereless Bodies of the Solar System

Zh. M. Dlugach[a] and M. I. Mishchenko[b]

[a] *Main Astronomical Observatory, National Academy of Sciences of Ukraine, Goloseevo, Kiev, 03680 Ukraine*
[b] *NASA Goddard Institute for Space Studies, 2880 Broadway, New York, NY, 10025 USA*

Received November 20, 2012

Abstract—The results of photometric and polarimetric observations carried out for some bright atmosphereless bodies of the Solar system near the zero phase angle reveal the simultaneous existence of two spectacular optical phenomena, the so-called brightness and polarization opposition effects. In a number of studies, these phenomena were explained by the influence of coherent backscattering. However, in general, the interference concept of coherent backscattering can be used only in the case where the particles are in the far-field zones of each other, i.e., when the scattering medium is rather rarefied. Because of this, it is important to prove rigorously and to demonstrate that the coherent backscattering effect may also exist in densely packed scattering media like regolith surface layers of celestial bodies. From the results of the computer modeling performed with the use of numerically exact solutions of the macroscopic Maxwell equations for discrete random media with different packing densities of particles, we studied the origin and evolution of all the opposition phenomena predicted by the coherent backscattering theory for low-packing-density media. It has been shown that the predictions of this theory remain valid for rather high packing densities of particles that are typical, in particular, of regolith surfaces of the Solar system bodies. The results allow us to conclude that both opposition effects observed simultaneously in some high-albedo atmosphereless bodies of the Solar system are caused precisely by coherent backscattering of solar light in the regolith layers composed of microscopic particles.

DOI: 10.1134/S0038094613060014

INTRODUCTION

The results of photometric and polarimetric observations carried out near the zero phase angle show that two unique optical phenomena, the so-called brightness and polarization opposition effects, are simultaneously present in some bright atmosphereless bodies of the Solar system. Figure 1 taken from the paper by Mishchenko et al. (2006a) displays the observational data acquired in the visible spectral range for the high-albedo asteroids 44 Nysa and 64 Angelina, the Jovian satellite Europa, and Saturn's rings (Franklin and Cook, 1965; Zellner and Gradie, 1976; Johnson et al., 1980; Harris et al., 1989; Thompson and Lockwood, 1992; Dollfus, 1996; Rosenbush et al., 2005; Rosenbush and Kiselev, 2005). It is seen that each of the photometric phase curves in the left part of the plot has a very narrow nonlinear peak centered at zero phase angle and superimposed on a linear background. This nonlinear peak of brightness is called the brightness opposition effect (BOE). In the right part of the plot, each of the phase dependencies of the degree of linear polarization demonstrates a narrow local minimum of negative polarization centered at a phase angle approximately equal to a half-width of the corresponding brightness peak. Each minimum is superposed on a broad, nearly parabolic branch of negative polarization that is characteristic of the majority of atmosphereless bodies of the Solar system. Such a narrow asymmetric minimum of negative polarization is called the polarization opposition effect (POE) (Mishchenko, 1993).

Shkuratov (1989) and Muinonen (1990) were the first who hypothesized that two optical effects observed in a wide class of atmosphereless bodies near opposition, namely BOE and the parabolic branch of negative polarization, are caused by coherent backscattering in discrete random media. However, it is known that the parabolic branch of negative polarization can be induced by both single scattering by nonspherical grains of the surface regolith layer and near-field effects (Petrova and Tishkovets, 2011). In the papers by Mishchenko (1993) and Mishchenko et al. (2000), it was concluded that coherent backscattering causes an extremely narrow asymmetric peak of negative polarization that appears if the incident radiation is nonpolarized. It was supposed that the BOE should be accompanied by the POE, if a substantial portion of the surface is covered by particles smaller than the wavelength, and the angle of the minimal negative polarization should be comparable to the BOE half-width.

In the papers by Mishchenko (1992a; 1992b), the rigorous relations allowed all the characteristics of the coherent backscattering effect to be calculated for the precise backscattering direction from the exact solution of the vector radiative transfer equation for the low-packing-density media composed of particles of

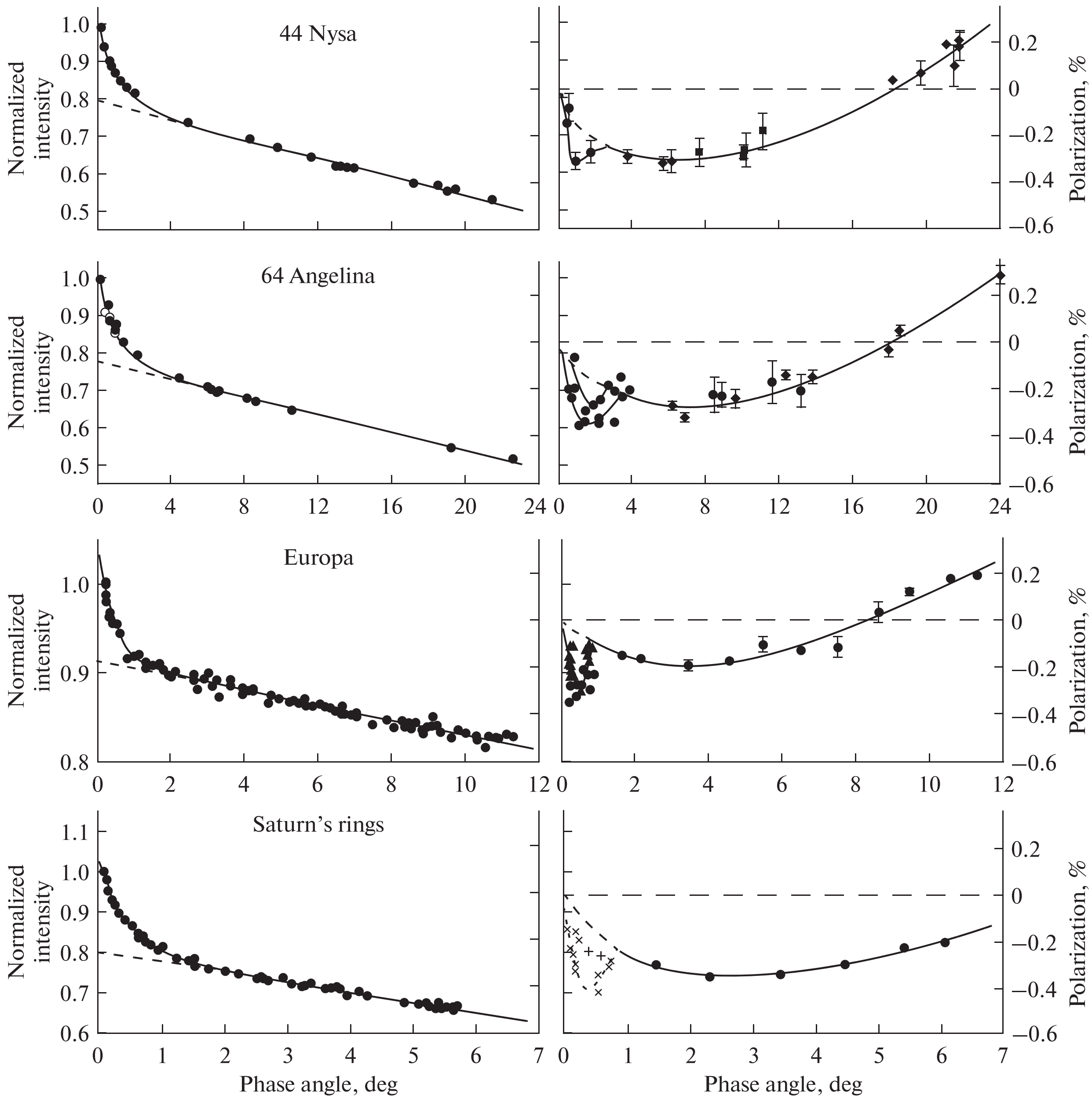

Fig. 1. The values of the normalized (to the minimal phase angle) intensity and the degree of linear polarization of light measured in the asteroids 44 Nysa and 64 Angelina, the satellite Europa, and Saturn's rings (Mishchenko et al., 2006a).

arbitrary shape and size. With the use of these relations, it was shown that the coherent backscattering effect in the regolith layers containing submicron particles with a refractive index of about 1.31 (for the satellite Europa and Saturn's rings) and 1.65 (for the high-albedo asteroids 44 Nysa and 64 Angelina) can be one of the causes of the observed brightness opposition effects (Mishchenko and Dlugach, 1992; 1993; Dlugach and Mishchenko, 1999). Moreover, this theory was successfully used (Mishchenko and Dlugach, 2008) in the interpretation of the radar polarization observations of Saturn's rings, namely, the results of measurements of the circular polarization ratios (Ostro et al., 1980; Nicholson et al., 2005).

However, the interference concept of the coherent backscattering effect is strictly applicable only when the particles are in the far scattering zone relative to each other, i.e., when the scattering medium is sufficiently sparse (the packing density of particles is negligible) (Barabanenkov et al., 1991; Mishchenko et al., 2006b). Therefore, one faces a question of whether the coherent backscattering effect can also take place in the case of densely packed media like regolith layers of the surfaces of celestial bodies. A definitive answer to this question can only be obtained from numerically

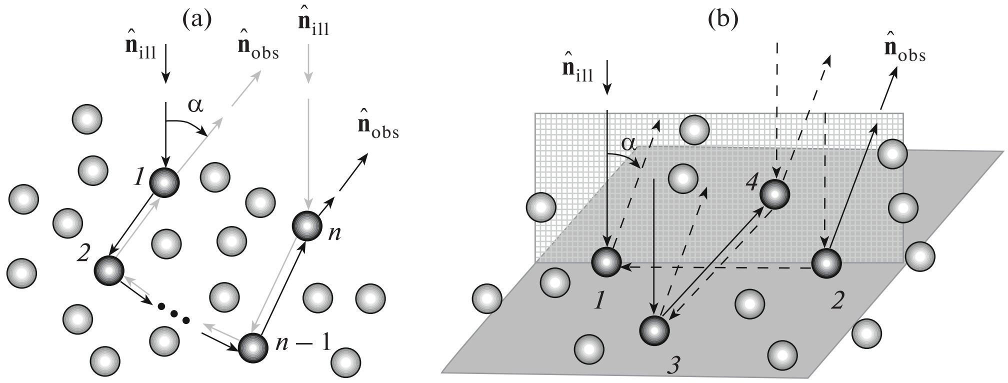

Fig. 2. Schematic explanation of the physical nature of the brightness and polarization opposition effects.

exact solutions of the macroscopic Maxwell equations for the media composed of varying numbers of randomly positioned particles. This approach allows, first, the uncertainties connected with the use of different approximations to be eliminated and, second, the influence of different parameters of the medium to be immediately controlled by individual varying of their values. Thus, one may study the evolution of all effects caused by coherent backscattering as the packing density of particles grows from zero to the values typical of the regolith surface layers, and the results obtained allow of a clear answer on the physical nature of the opposition effects observed.

THEORY

The effect of coherent backscattering (or weak localization) of electromagnetic waves in discrete random media predicted by Watson (1969) in the study of multiple scattering of electromagnetic waves in a rarefied plasma still remains the subject of active theoretical and laboratory researches (see, e.g., Akkermans et al., 1988; van der Mark et al., 1988; Barabenkov et al., 1991; Kuz'min and Romanov, 1996; Mishchenko et al., 2006b). To explain the interference nature of the coherent backscattering effect, let us consider a discrete medium composed of randomly positioned scattering particles illuminated by a plane wave incident in the direction specified by the unit vector $\hat{\mathbf{n}}_{\text{ill}}$ (Fig. 2a). Let the direction of the scattered wave be determined by the unit vector $\hat{\mathbf{n}}_{\text{obs}}$, and the observer be very far from the medium. Consider two reverse (conjugate) scattering paths involving the same configuration of *N* particles. The waves scattered through these paths will interfere, and the interference is constructive or destructive depending on the phase difference between the paths. If the observer is sufficiently far from the exact backscattering direction ($-\hat{\mathbf{n}}_{\text{ill}}$), the average effect of interference of the conjugate scattered waves going through a group of particles in opposite directions is zero, owing to the randomness of particle positions. Consequently, the observer measures some incoherent (diffuse) intensity. However, at $\alpha = 0°$ ($\hat{\mathbf{n}}_{\text{obs}} = -\hat{\mathbf{n}}_{\text{ill}}$), the phase difference between the conjugate paths involving any configuration of particles is identically equal to zero, i.e., the coherence completely remains, and the interference is always constructive. It is this effect that induces the opposition peak in the intensity of the scattered radiation.

To explain the nature of the polarization opposition effect, let us consider particles *1*–*4* lying in a plane normal to the illumination direction (Fig. 4b) and assume that their sizes are much smaller than the wavelength (Shkuratov, 1989; Muinonen, 1990). Particles *1* and *2* lie in the scattering plane, while particles *3* and *4* are in the perpendicular plane. If the incident radiation is unpolarized, then it can be represented as a mixture of two linearly polarized beams of light with mutually perpendicular directions of the polarization planes. Light scattered along conjugate paths involving particles *3* and *4* is negatively polarized, while scattering along the paths involving particles *1* and *2* yields positive polarization. In the first case, the phase difference between the conjugate paths is always zero, while in the second case it is zero only at $\alpha = 0°$ and oscillates rapidly with increasing α. Therefore, on average, coherent backscattering enhances the contribution of negative polarization over a wider range of phase angles. The result is the negative polarization minimum at a small phase angle (POE) comparable to the angular width of the coherent intensity peak (BOE). The fact that only certain particle configurations contribute to the POE often makes the latter less pronounced than the BOE.

Apparently, the POE was observed for the first time in laboratory by Lyot (1929), when he measured the degree of polarization of a powder-like surface composed of microscopic MgO particles. The author called the measured narrow minimum of negative polarization mysterious and attributed its existence to extremely small sizes of magnesium oxide particles. In the study by Shkuratov et al. (2002), these results were successfully reproduced and supplemented by photometric measurements that showed the simultaneous presence of a narrow BOE.

The interference explanation of the coherent backscattering effect relies on the notion of phase of an electromagnetic wave. In this connection, it is important to stress that the notion of phase itself is applicable only to transverse electromagnetic waves, such as a plane or spherical wave. Due to this, the interference explanation of the coherent backscattering effect indirectly relies on the assumption that each of the particles in any sequence of particles (Fig. 2a) is in the far-field scattering zones of both the previous particle and the next one. Therefore, in order to justify the involvement of the concept of coherent backscattering for explaining the observational data acquired for densely packed media, the range of applicability of the coherent backscattering theory should be clearly determined. This can be done on the basis of the results of the numerically exact solution of the macroscopic Maxwell equations for scattering media with a varied packing density of particles. Such computations have become possible only recently due to the development of effective numerical methods and the increase of the computer power (especially, due to the ever-increasing power of computers (Mackowski and Mishchenko, 2011; and references therein)).

THE TECHNIQUE OF NUMERICALLY EXACT MODELING OF LIGHT SCATTERING BY A MEDIUM WITH AN ARBITRARY PACKING DENSITY OF PARTICLES

To examine with numerically exact calculations whether the use of the coherent backscattering theory is valid for densely packed media, an adequate model of the scattering medium should, first of all, be chosen. As such a model, let us consider an imagined spherical volume of radius R filled with N randomly positioned nonoverlapping spherical particles of radius r (see Fig. 3). The size parameter of the scattering volume and each of the particles is kR and kr, respectively, where k is the wave number in vacuum. To model the statistically random particle positions within the spherical volume consistent with the fundamental assumption of ergodicity (i.e., for a specified realization of a random scattering process, the average over time is equivalent to the average over an ensemble (Mishchenko et al., 2006b)), we follow the approach pioneered by Mishchenko et al. (2007). Specifically, we use one realization of an N-particle group generated randomly according to the algorithm by Mackowski (2006) and then average all scattering characteristics over the uniform orientation distribution of this configuration with respect to the laboratory coordinate system. The result is an infinite continuous set of random realizations of the N-particle group, which enables one to use the efficient orientation averaging technique developed in the framework of the superposition T-matrix method (Mackowski and Mishchenko, 1996; Mishchenko et al., 2002).

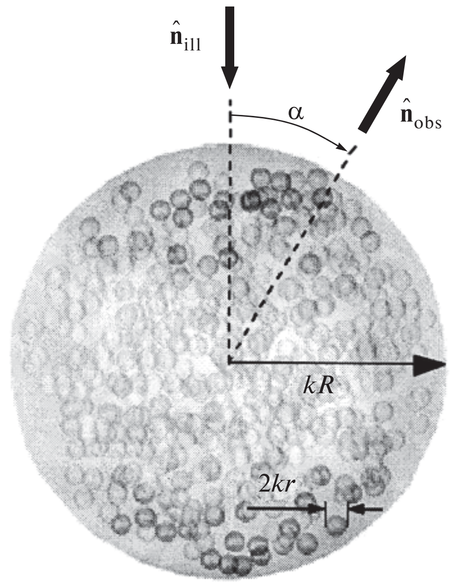

Fig. 3. Schematic explanation of the light scattering process in a macroscopic spherical volume filled with N nonoverlapping randomly positioned spherical particles.

It is obvious that the adopted model cannot reproduce the infinite diversity of the particulate media morphologies encountered in natural conditions and in the laboratory. However, it proves to be sufficiently representative to permit a clear pattern of the effects of packing density on light scattering by a discrete random medium.

Assume that the statistically random particulate volume is illuminated by a parallel quasi-monochromatic beam of light propagating in the direction of the unit vector $\hat{\mathbf{n}}_{\rm ill}$ and the observer is located in the far-field zone of the entire scattering volume in the direction $\hat{\mathbf{n}}_{\rm obs}$ (Fig. 3). Since the scattering properties of the volume are averaged over all orientations of the N-particle random configuration, they depend only on the scattering angle θ (or the phase angle $\alpha = \pi - \theta$) provided that the scattering plane is used for defining the Stokes parameters of the incident and scattered light.

In the far-field zone, the Stokes parameters for the incident and scattered radiation are related as (Mishchenko et al., 2006b)

$$\begin{bmatrix} I^{sca} \\ Q^{sca} \\ U^{sca} \\ V^{sca} \end{bmatrix} \propto \mathbf{F}(\alpha) \begin{bmatrix} I^{inc} \\ Q^{inc} \\ U^{inc} \\ V^{inc} \end{bmatrix}$$
$$\propto \begin{bmatrix} a_1() & b_1(\alpha) & 0 & 0 \\ b_1(\alpha) & a_2(\alpha) & 0 & 0 \\ 0 & 0 & a_3(\alpha) & b_2(\alpha) \\ 0 & 0 & -b_2(\alpha) & a_4(\alpha) \end{bmatrix} \begin{bmatrix} I^{inc} \\ Q^{inc} \\ U^{inc} \\ V^{inc} \end{bmatrix}. \quad (1)$$

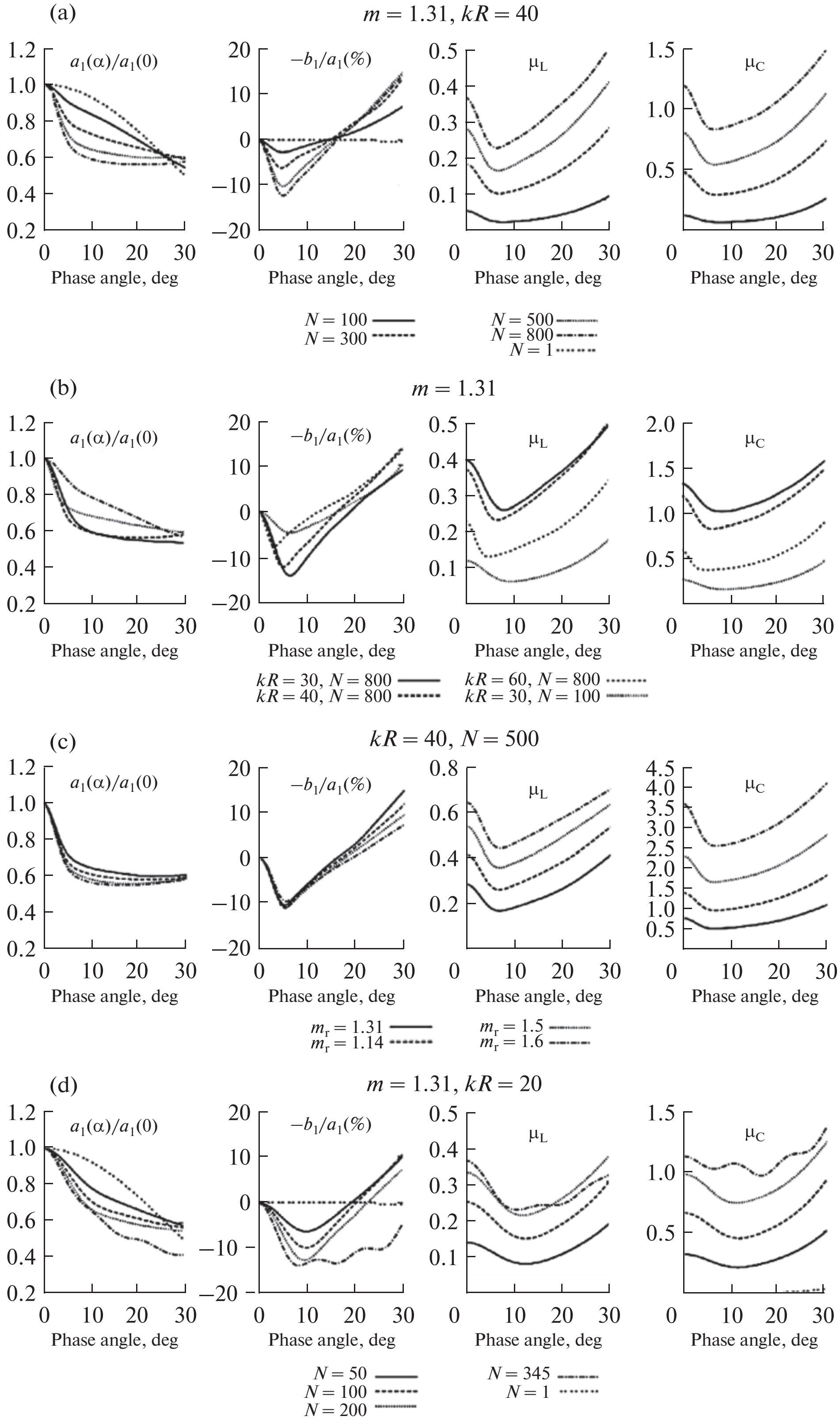

Fig. 4. The scattering characteristics calculated for spherical volumes randomly filled with spherical particles.

The scattering matrix $\mathbf{F}(\alpha)$ is a special case of the Mueller transformation matrix (Hovenier et al., 2004). Strictly speaking, the elements of the matrix $\mathbf{F}(\alpha)$ denoted in Eq. (1) by zeros vanish only if the primordial N-sphere configuration had a plane of symmetry. Our calculations showed, however, that in all cases considered below the magnitudes of these matrix elements are much smaller than those of the other elements in absolute value. In other words, the zeros denote the matrix elements that are negligibly small (in an absolute sense) relative to the other elements at the same scattering angles.

From the scattering matrix elements, the conventional optical characteristics, corresponding to different types of polarization state of the incident radiation, can be calculated. Specifically, if the incident light is unpolarized, the first element $a_1(\alpha)$ (the phase function) determines the angular distribution of the intensity of the scattered radiation in the far field, while the ratio $-b_1(\alpha)/a_1(\alpha)$ gives the corresponding degree of linear polarization. If the incident radiation is polarized linearly in the scattering plane, the linear polarization ratio is defined as

$$\mu_L = \frac{a_1(\alpha) - a_2(\alpha)}{a_1(\alpha) + 2b_1(\alpha) + a_2(\alpha)}. \qquad (2)$$

If the incident radiation is polarized circularly in the counterclockwise direction, when looking in the direction of propagation, the circular polarization ratio is

$$\mu_C = \frac{a_1(\alpha) + a_4(\alpha)}{a_1(\alpha) - a_4(\alpha)}. \qquad (3)$$

It is worth stressing that the degree of linear polarization of light singly scattered by one particle (for unpolarized incident light) may have a negative branch in the range of phase angles from 0° to 20°. In such cases, a direct computer modeling of the POE can be quite problematic, since it is impossible to distinguish between the singly and multiply scattered contributions in a direct numerical solution of the Maxwell equations (Mishchenko et al., 2007; Petrova et al., 2007). In order to eliminate this uncertainty, the following technique was suggested (Mishchenko et al., 2009a). For each value of the considered refractive index, we select a size parameter value kr yielding a single-scattering contribution with near-zero values in a wide interval at small phase angles. This allows the multiple-scattering contribution to be unambiguously distinguished and qualitatively estimated. Note that this approach made it possible to demonstrate for the first time, with the use of numerically exact computer solutions of the Maxwell equations, the whole set of optical effects predicted by the low-density theory of coherent backscattering (Mishchenko et al., 2009a; 2009b; Dlugach et al., 2011).

Different optical characteristics of the scattering volumes containing both nonabsorbing and absorbing particles were calculated with the superposition T-matrix method (Mackowski and Mishchenko, 1996; 2011). The cases of polydisperse scattering media composed of particles of different sizes or different chemical composition were also considered. Here, we will only briefly review the results obtained for the scattering volumes with the size parameter kR ranging from 20 to 60. The volumes are filled with nonabsorbing spherical particles; several values of the real refractive index were considered: $m = m_r = 1.194$ (latex in water), 1.31 (water droplets or ice in the visible spectral range), 1.4, 1.5, and 1.6 (different minerals). Depending on the value of kR, the number of particles N was varied; and $N_{max} = 900$ for $kR = 30$.

Figure 4a illustrates the results of our calculations for the phase range $0° \le \alpha \le 30°$. They were performed for $m = 1.31$, $kR = 40$, $kr = 2$, and the packing density $\tilde{\rho}$, changing from 1.5% ($N = 100$) to 11.7% ($N = 800$). For comparison, we also show the data corresponding to the scattering by a single particle. It is seen that the results of a numerically exact solution of the Maxwell equations completely agree with the qualitative predictions of the low-density theory of coherent backscattering, namely:

(1) The normalized intensities of the scattered radiation $a_1(\alpha)/a_1(0°)$ exhibit the backscattering peaks rapidly developing with N, and the angular width of these peaks remains practically the same.

(2) In the phase-angle range from $0° \le \alpha \le 30°$, the degree of linear polarization $-b_1(\alpha)/a_1(\alpha)$ is equal to zero for $N = 1$, but rapidly develops a pronounced minimum with growing N caused by the increasing contribution from multiple-scattering; the phase angle of the polarization minimum α_{min} is virtually independent of N and is comparable to the angular width of the peak of the normalized intensity $a_1(\alpha)/a_1(0°)$. Furthermore, the angular shape of the branch of negative polarization is asymmetric, with α_{min} being significantly closer to zero than to the inversion phase angle.

In order to analyze the dependence of the optical characteristics on the size parameter of the scattering volume kR, the results of calculations for $m = 1.31$, $N = 800$, and $kR = 30$, 40, and 60 are shown in Fig. 4b. It is seen that the angular width of all peaks and the angle of the polarization minimum decrease with increasing kR approximately as $1/kR$.

In Fig. 4c, the results of calculations for the constant value of the size parameter $kR = 40$ and the monomer number $N = 500$, and for the refractive indexes $m = 1.31$, 1.4, 1.5, and 1.6 are presented. One can easily see similar opposition effects for all refractive index values, which illustrates the interference nature of the coherent backscattering effect.

From Figs. 4a–4c, we may conclude that all of the peculiarities in the behavior of the peaks of normalized intensity and polarization minimum confirm their interference origin caused by multiple scattering. Specifically, the peaks of intensity of the scattered radiation and the minima of negative polarization are absent in the case of a single particle, but appear for the scattering volumes with $N > 1$. The angular width of the normalized intensity peak is comparable to the phase angle $\alpha_{\min}$, and both of them are independent of N and m and are inversely proportional to the size parameter of a scattering volume kR. Furthermore, the polarization minima become increasingly asymmetric with increasing kR. The opposition peaks of intensity appear and develop with increasing N due to the influence of the multiple-scattering contribution, and their angular widths are inversely proportional to kR, which once again confirms their interference origin. For a fixed kR, the angular widths of the peaks are approximately the same and are independent of the number of particles and their refractive index, though the peak amplitudes increases with increasing refractive index.

The linear μ_L and circular μ_C polarization ratios calculated with Eqs. (2) and (3) can serve as an even better illustration of the origin and evolution of the coherent backscattering effect, since they coincide with the abscissa axis for a single particle. The backscattering peaks appear and grow with increasing N under the influence of the multiple-scattering contribution, and their angular widths are inversely proportional to kR, which is indicative of their interference origin. For a fixed kR, the angular width is practically independent of the number of particles and their refractive index, though the peak height increases with increasing refractive index.

The effect of increasing the number of particles in the scattering volume can be expected to be twofold. Initially, it simulates multiple scattering and thus enhances the classical manifestations of diffuse and coherent scattering of light. Eventually, however, the increased number of particles can cause changes in the scattering characteristics of the whole volume not implied by the classical theories of radiative transfer and coherent backscattering. One should, therefore, expect that the analysis of the numerically exact T-matrix results with the use of these theories becomes inadequate, when the packing density of particles increases to rather large values.

In order to analyze the effect of increasing the number of particles N on the scattering properties of the volume in the backscattering direction, we consider the results of calculations carried out for $kR = 20$, $m = 1.31$, $kr = 2$, and N varied from 50 ($\tilde{\rho} \sim 7\%$) to 345 ($\tilde{\rho} \sim 47\%$) (Fig. 4d). We see that, indeed, (as the calculations showed, the effect appears starting from $N = 300$ ($N = 300$ ($\tilde{\rho} \sim 41\%$)) the curves develop interference ripples typical of a single spherical particle with a radius substantially larger than the wavelength (calculations performed for $kR = 31$ show a similar result (Mackowski and Mishchenko, 2011)). Obviously, such a behavior of all of the considered optical characteristics is not predicted by the coherent backscattering theory valid for low-density media. Nevertheless, the results of our computations do demonstrate that the predictions of this theory can survive relatively high packing densities of particles typical, in particular, of the regolith surfaces of Solar system bodies. It is worth noting that the recent results (Muinonen et al., 2012) obtained with the Monte-Carlo technique for calculations of the diffuse and coherent components according to the microphysical theory of radiative transfer and coherent backscattering (Mishchenko et al., 2006b) confirm this statement.

Our results of the numerically exact modeling performed for the media with different packing densities pose a question as to why the manifestations of the coherent backscattering effect are so remarkably immune to the increase of the packing density of particles. This can be caused by the fact that, even in relatively densely packed media, the partial wavelets scattered by sequences of widely separated particles still provide a sufficient contribution to the total scattered radiation and, thereby, make the classical coherent backscattering features quite pronounced.

CONCLUDING REMARKS

It must be emphasized once again that the results of computations presented above were obtained for a relatively simple model of a scattering medium. Moreover, one should have in mind that the disk-integrated observations of the celestial bodies having the heterogeneous surfaces yield cumulative information on the contribution of morphologically different surface areas with different values of albedo. Some of them may induce the BOE and POE with varying angular width and amplitude, while the others may cause only the BOE changing over the surface. These factors make the prospects of unambiguous interpretation of such observational data, especially with the direct solution of the Maxwell equations in terms of the refractive index, size, and packing density of particles, to be extremely problematic. Nevertheless, the possibility of the presence of the coherent backscattering effect in rather densely packed media confirmed by our modeling allows the opposition effects observed in a number of high-albedo atmosphereless bodies of the Solar system (Fig. 1) to be reliably explained.

The calculated values of the opposition peak amplitude in intensity of radiation and the opposition minimum depth in polarization (Figs. 4a, 4c) are larger than the corresponding values measured in the high-albedo asteroids and planetary satellites (Rosenbush and Mishchenko, 2011). This difference would be expected, since it is highly improbable that the entire surface of these celestial bodies is covered by identical microscopic grains inducing the spatially constant BOE and POE. The measured angular width of the opposition effects turns out to be substantially smaller than the calculated one, which can be explained by the fact that the interference base for a finite scattering volume is determined by its size parameter kR, while for the optically thick nonabsorbing or weakly absorbing regolith layer it is controlled by the product $k\lambda_{tr}$, where λ_{tr} is the transport free path (Barabanenkov et al., 1991). The actual values of $k\lambda_{tr}$ may substantially exceed the kR values used in our computations, thereby resulting in much narrower opposition effects observed. Note that the Monte-Carlo calculations (Muinonen et al., 2012) showed that the substantial increase of the size of a scattering volume really causes the considerable decrease of the angular width of the opposition peaks.

In conclusion, we stress that the photometric and polarimetric observations of the asteroids 44 Nysa and 64 Angelina, the satellite Europa, and Saturn's rings (Fig. 1) are unique in that they reveal simultaneous existence of the brightness and polarization opposition effects of nearly equal angular widths and angular profiles consistent with the exact solutions of the Maxwell equations (Fig. 4). Up to now, no other theory directly based on the Maxwell equations, except the coherent backscattering theory, has predicted both these effects simultaneously. Therefore, our numerically exact results allow of the conclusion that both opposition effects are caused by coherent backscattering of solar light in the regolith layers composed of microscopic ice (for the satellite Europa and Saturn's rings) and silicate (for the asteroids 44 Nysa and 64 Angelina) particles.

ACKNOWLEDGMENTS

The work was supported by the National Academy of Sciences of Ukraine under the Main Astronomical Observatory GRAPE/GPU/GRID computing cluster project. The authors are grateful to the referee for a valuable comment.

REFERENCES

Akkermans, E., Wolf, P., Maynard, R., and Maret, G., Theoretical study of the coherent backscattering of light by disordered media, *J. Phys. (Paris),* 1988, vol. 49, pp. 77–98.

Barabanenkov, Yu.N., Kravtsov, Yu.A., Ozrin, V.D., and Zaichev, A.I., Enhanced backscattering in optics, *Prog. Opt.*, 1991, vol. 29, pp. 65–197.

Dlugach, J.M. and Mishchenko, M.I., Coherent backscatter as one of the possible mechanisms of forming the opposition brightness peak for some bodies of the solar system, *Sol. Syst. Res.*, 1999, vol. 33, pp. 472–481.

Dlugach, J.M., Mishchenko, M.I., Liu, L., and Mackowski, D.W., Numerically exact computer simulations of light scattering by densely packed, random particulate medium, *J. Quant. Spectrosc. Radiat. Transf.,* 2011, vol. 112, pp. 2068–2078.

Dollfus, A., Saturn's rings: optical reflectance polarimetry, *Icarus,* 1996, vol. 124, pp. 237–261.

Franklin, F.A. and Cook, A.F., Optical properties of Saturn's rings. II. Two-color phase curves of the two bright rings, *Astron. J.*, 1965, vol. 70, pp. 704–720.

Harris, A.W., Young, J.W., Contreiras, L., et al., Phase relations of high albedo asteroids: the unusual opposition brightening of 44 Nysa and 64 Angelina, *Icarus*, 1989, vol. 81, pp. 365–374.

Hovenier, J.W., van der Mee, C., and Domke, H., *Transfer of Polarized Light in Planetary Atmospheres—Basic Concepts and Practical Methods*, Berlin: Springer, 2004.

Johnson, P.E., Kemp, J.C., King, R., et al., New results from optical polarimetry of Saturn's rings, *Nature*, 1980, vol. 283, pp. 146–149.

Kuz'min, V.L. and Romanov, V.P., Reviews of topical problems: coherent phenomena in light scattering from disordered systems, *Phys.-Usp.*, 1996, vol. 39, pp. 231–260.

Lyot, B., Recherche sur la polarization de la lumiere des planets et de quelques substances terrestres, *Ann. Obs. Meudon VIII*, 1929, vol. 1, pp. 1–161.

Mackowski, D.W., A simplified model to predict the effects of aggregation on the absorption properties of soot particles, *J. Quant. Spectrosc. Radiat. Transf.*, 2006, vol. 100, pp. 237–249.

Mackowski, D.W. and Mishchenko, M.I., A multiple sphere T-matrix fortran code for use on parallel computer clusters, *J. Quant. Spectrosc. Radiat. Transf.,* 2011., vol. 112, pp. 2182–2192.

Mackowski, D.W. and Mishchenko, M.I., Calculation of the *T* matrix and the scattering matrix for ensembles of spheres, *J. Opt. Soc. Am. A,* 1996, vol. 13, pp. 2266–2278.

Mishchenko, M.I., Enhanced backscattering of polarized light from discrete random media: calculation in exactly the backscattering direction, *J. Opt. Soc. Am. A*, 1992b, vol. 9, pp. 978–982.

Mishchenko, M.I., On the nature of the polarization opposition effect exhibited by Saturn's rings, *Astrophys. J.,* 1993b, vol. 411, pp. 351–361.

Mishchenko, M.I., Polarization characteristics of the coherent backscatter opposition effect, *Earth, Moon Planets*, 1992c, vol. 58, pp. 127–144.

Mishchenko, M.I. and Dlugach, J.M., Can weak localization of photons explain the opposition effect of Saturn's rings, *Mon. Notic. Roy. Astron. Soc.*, 1992a, vol. 254, pp. 15P–18P.

Mishchenko, M.I. and Dlugach, J.M., Coherent backscatter and the opposition effect for E-type asteroids, *Planet. Space Sci.*, 1993a, vol. 41, pp. 173–181.

Mishchenko, M.I. and Dlugach, J.M., Weak localization of electromagnetic waves and radar polarimetry of Saturn's rings, *Mon. Notic. Roy. Astron. Soc.,* 2008, vol. 389, pp. 1665–1674.

Mishchenko, M.I., Dlugach, J.M., and Liu, L., Azimuthal asymmetry of the coherent backscattering cone: theoretical results, *Phys. Rev. A*, 2009b, vol. 80, pp. 053824-1–053824-10.

Mishchenko, M.I., Dlugach, J.M., Liu, L., et al., Direct solutions of the Maxwell equations explain opposition phenomena observed for high-albedo solar system objects, *Astrophys. J.,* 2009a, vol. 705, pp. L118–L112.

Mishchenko, M.I., Liu, L., Mackowski, D.W., et al., Multiple scattering by random particulate medium: exact 3D results, *Opt. Express*, 2007, vol. 15, pp. 2822–2836.

Mishchenko, M.I., Luck, J.M., and Nieuwenhuizen, T.M., Full angular profile of the coherent polarization opposition effect, *J. Opt. Soc. Am. A,* 2000, vol. 17, pp. 888–891.

Mishchenko, M.I., Rosenbush, V.K., and Kiselev, N.N., Weak localization of electromagnetic waves and opposition phenomena exhibited by high-albedo atmosphereless Solar system objects, *Appl. Opt.*, 2006a, vol. 45, pp. 4459–4463.

Mishchenko, M.I., Travis, L.D., and Lacis, A.A., *Multiple Scattering of Light by Particles: Radiative Transfer and Coherent Backscattering*, Cambridge: Cambridge Univ. Press, 2006b.

Mishchenko, M.I., Travis, L.D., and Lacis, A.A., *Scattering, Absorption, and Emission of Light by Small Particles*, Cambridge: Cambridge Univ. Press, 2002.

Muinonen, K., Light scattering by inhomogeneous media: backward enhancement and reversal of polarization, *Ph.D. Thesis*, Helsinki: Univ. Helsinki, 1990.

Muinonen, K., Mishchenko, M.I., Dlugach, J.M., et al., Coherent backscattering verified numerically for a finite volume of spherical particles, *Astrophys. J.*, 2012, vol. 760. doi: 10.1088/0004-637X/760/2/118

Nicholson, P.D., French, R.G., Campbell, D.B., et al., Radar imaging of Saturn's rings, *Icarus*, 2005, vol. 177, pp. 32–62.

Ostro, S.J., Pettengill, G.H. and Campbell, D.B., Radar observations of Saturn's rings at intermediate tilt angles, *Icarus*, 1980, vol. 41, p. 381–388.

Petrova, E.V., Tishkovets, V.P., and Jockers, K., Modeling of opposition effects with ensembles of clusters: interplay of various scattering mechanisms, *Icarus*, 2007, vol. 188, pp. 233–245.

Petrova, E.V. and Tishkovets, V.P., Light scattering by morphologically complex objects and opposition effects (a review), *Sol. Syst. Res.*, 2011, vol. 45, no. 4, pp. 304–322.

Rosenbush, V.K. and Kiselev, N.B., Polarization opposition effect for the Galilean satellites of Jupiter, *Icarus,* 2005a, vol. 179, pp. 490–496.

Rosenbush, V.K., Kiselev, N.N., Shevchenko, V.G., et al., Polarization and brightness opposition effects for the E-type asteroid 64 Angelina, *Icarus*, 2005b, vol. 178, pp. 222–234.

Rosenbush, V.K. and Mishchenko, M.I., Opposition planetary phenomena in planetary astrophysics: observational results, in *Polarimetric Detection, Characterization, and Remote Sensing*, Mishhchenko, M.I., Yatskiv, Ya.S., Rosenbush, V.K., and Videen, G., Eds., Dordrecht: Springer, 2011.

Shkuratov, Y.G., A new mechanism of formation of negative polarization of light scattered by the solid surfaces of cosmic bodies, *Sol. Syst. Res.,* 1989, vol. 23, pp. 111–115.

Shkuratov, Yu., Ovcharenko, A., Zubko, E., et al., The opposition effect and negative polarization of structural analogs for planetary regoliths, *Icarus*, 2002, vol. 159, pp. 396–416.

Thompson, D.T. and Lockwood, G.W., Photoelectric photometry of Europa and Callisto, *J. Geophys. Res.*, 1992, vol. 97, pp. 14761–14772.

van der Mark, M.V., van Albada, M.P., and Lagendijk, A., Light scattering in strongly scattering media: multiple scattering and weak localization, *Phys. Rev.,* 1988, vol. 37, pp. 3575–3592.

Watson, K.M., Multiple scattering of electromagnetic waves in an underdense plasma, *J. Math. Phys.*, 1969, vol. 10, pp. 688–702.

Zellner, B. and Gradie, J., Minor planets and related objects. XX. Polarimetric evidence for the albedos and compositions of 94 asteroids, *Astron. J.*, 1976, vol. 81, pp. 262–280.

Translated by E. Petrova